

Exhibit 5

Conditional cell ablation by tight control of caspase-3 dimerization in transgenic mice

Vincent O. Mallet^{1†}, Claudia Mitchell^{1†}, Jacques-Emmanuel Guidotti¹, Patrick Jaffray², Monique Fabre³, David Spencer⁴, Damien Arnoult⁵, Axel Kahn¹, and Hélène Gilgenkrantz^{1*}

Published online 18 November 2002; doi:10.1038/nbt762

Studying the effects of the loss of a specific cell type is a powerful approach in biology. Here we present a method based on the controlled activation of the apoptotic machinery. We expressed a modified caspase-3-containing chemical inducer of dimerization (CID)-binding sites in the livers of transgenic mice. In the absence of CID, no liver injury was detectable, underlining the absence of leakage in our system. In contrast, injection of the CID produced activation of the chimeric caspase-3, which led to a dose-dependent pure hepatocyte ablation with subsequent regeneration. This method is effective in both growing and nongrowing cells, and is therefore applicable to a wide range of cells and tissues. Moreover, because apoptosis has been described in numerous pathological circumstances, this system is useful for generating mouse models of human disorders as well as for studying the recovery or regeneration of tissues after cell loss.

Apoptosis is an active and highly regulated form of cell death that has been described in several causes of acute liver injury (ALI), including viral hepatitis¹, alcoholic hepatitis², and primary biliary cirrhosis³ as well as metabolic⁴, ischemic⁵, and toxic liver injury⁶. ALI can ultimately lead to fulminant hepatic failure (FHF)^{7–9}, depending on the extent of functional hepatic compromise and the ability of undamaged hepatocytes to regenerate the diseased parenchyma. In this situation, the only effective treatment is whole-liver transplantation. Unfortunately, this treatment has limitations, most notably the shortage of healthy donor livers.

Alternative therapeutic strategies relying on liver regeneration and hepatocyte transplantation have been proposed to bypass the need for a liver transplant^{10–13}. However, the development of these promising therapeutic options has been hampered by the lack of suitable animal models of ALI¹⁴. The most widely used models involve either the injection of a hepatotoxin or a surgical procedure. Disadvantages of these techniques include poor reproducibility, extrahepatic toxic side effects, a need for surgical expertise, and, for the most part, a lack of clinical relevance.

An alternative approach is to target suicide genes to control cell ablation. One method uses cell-specific expression of the diphtheria toxin-A (DT-A) subunit^{15,16}. However, this 'toxigene' approach is highly dependent on the tissue specificity of the promoter used and limited by the lack of temporal control over cell death. The most common approach for conditional cell ablation is based on expression of the gene encoding herpes simplex thymidine kinase (*HSVtk*)¹⁷, in which cell damage is caused by the administration of a nucleoside analog, ganciclovir¹⁸. In this model, a bystander effect alters the growth and proliferation of nearby viable tissue¹⁹. Another approach consists in the targeted expression of a specific receptor of toxins²⁰ or immunotoxins²¹. For example, a human receptor that

binds DT allows for considerable hepatotoxicity in response to a dose of DT that has no effect on wild-type mice²⁰. In these models, toxicity relies on the strong inhibition of protein synthesis²², a situation that has no clinical equivalent.

Our goal here was to develop a model of hepatocyte ablation that is devoid of liver regeneration impairment and based on a physiological intracellular signaling pathway. As apoptosis has been implicated in hepatitis of various origins, we have created a transgenic mouse model of inducible hepatic injury using hepatocyte-specific targeting of an inducible, dimerizable caspase-3 (ref. 23). There was no leakiness of the system. Upon activation, pure, dose-dependent hepatocyte ablation was observed with subsequent regeneration. Hepatic lesions ranged from simple hepatitis to FHF followed by an intensive regeneration process. This model offers new opportunities to study liver regeneration and stem cell plasticity. It also provides an effective approach to study apoptosis *in vivo* and to test therapeutic strategies in FHF. Finally, this method could provide a more general means to develop mouse models of human disorders.

Results

Generation of transgenic mice expressing human caspase-3 fused to dimerizable domains. The transgene includes a 3 kilobase mouse transthyretin (TTR) promoter sequence²⁴ driving the human myristoylated procaspase-3 (Casp3) fused to two modified domains of FKBP (M-F₂-Casp3). The construction and the mechanism of caspase-3 activation by the chemical inducer of dimerization (CID) are schematized in Figure 1A. After standard microinjection of the linearized construct, four independent transgenic founder mice were obtained. Each line expressed the M-F₂-Casp3 chimeric protein at different levels (Fig. 1B). Northern blot analysis of various tissues confirmed the liver-specific expression of M-F₂-Casp3 in transgenic lines

¹Department of Genetics, Development and Molecular Pathology, Cochin Institute, 24 rue du Faubourg Saint Jacques, 75014 Paris, France. ²Laboratory of Biochemistry, Cochin Hospital, 27 rue du Faubourg Saint Jacques, 75014, Paris, France. ³Laboratory of Pathology, Bichat Hospital, 78 rue du Général Leclerc, 94275 Le Kremlin-Bicêtre, France. ⁴Department of Immunology, Baylor College of Medicine, Houston, TX 77030. ⁵EMI-U 9922 INSERM, Bichat-Claude Bernard Hospital, 46, rue Henri Huchard, 75877 Paris cedex 18, France. *Corresponding author (gilgenkrantz@cochin.inserm.fr). [†]These two authors contributed equally to this work.

Exhibit 5

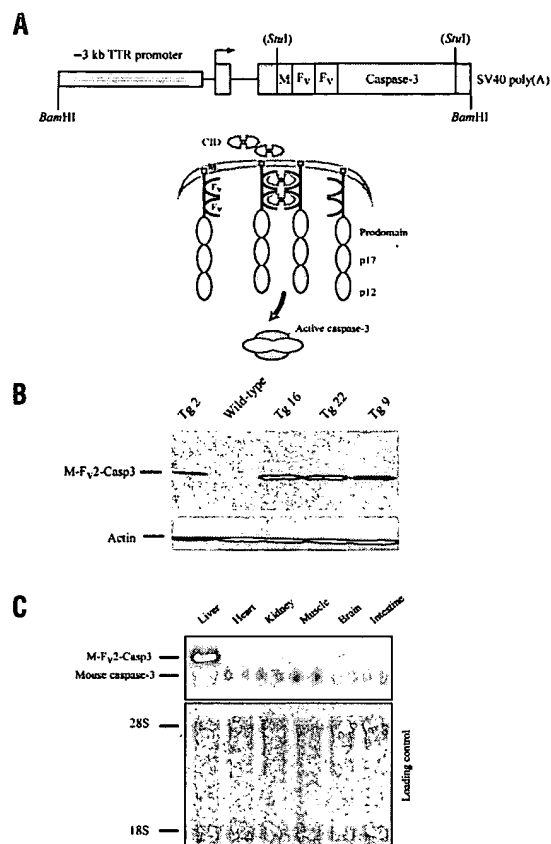


Figure 1. Construction, mechanism of caspase-3 activation, and analysis of transgenic animals. (A) Schematic representations of the transgenic construct and the CID strategy. The 3 kb mouse transthyretin promoter (TTR) and simian virus-40 (SV40) polyadenylation sequences are represented by black boxes. TTR first exon and part of the noncoding second exon (gray boxes) are separated by an intron (line). The arrow indicates the initiation of transcription. Human procaspase-3 cDNA is preceded by two CID-binding sites (Fv) and a myristoylation sequence (M). The chimeric procaspase-3 is anchored at the membrane by the myristoylation sequence (M). These proteins are brought in close proximity by the addition of the CID, which will induce their self-activation through internal proteolysis. Two small (p12) and two large (p17) subunits will associate to form the active heterotetrameric enzyme. (B) Western blot analysis of liver samples using an anti-human caspase-3 antibody. Representative animals of the four transgenic lines are shown. β -Actin is used as an internal control of the loaded amounts of liver proteins. (C) Northern blot analysis of transgenic organs for the expression of human chimeric caspase-3 (M-Fv2-Casp3). The endogenous murine caspase-3 (mouse caspase-3) is also detected. Methylene blue staining of the membrane before hybridization shows that equal amounts of total RNA were loaded in each lane. The tested organs are mentioned above.

(Fig. 1C). The transgene was specifically expressed in hepatocytes and not in endothelial or biliary epithelial cells either before or after CID injection, as assessed by immunohistochemistry (Fig. 2A). No abnormality was detected in transgenic animals in the absence of CID (Fig. 2B). Before induction, alanine aminotransferase (ALT) enzymatic activity, a sensitive and specific marker of liver injury, was normal compared to nontransgenic littermates (mean \pm s.d., 30 ± 14 ; $n = 8$).

Hepatocyte-specific ablation in transgenic mice upon injection of a CID. In this study, we have used a second-generation dimerizer, AP20187 (ARIAD Pharmaceuticals), derived from FK1012 (a semi-synthetic dimer of the natural product FK506)²⁵. We administered a single 2 mg/kg dose of AP20187 intraperitoneally to transgenic and nontransgenic animals and monitored liver injury by measuring

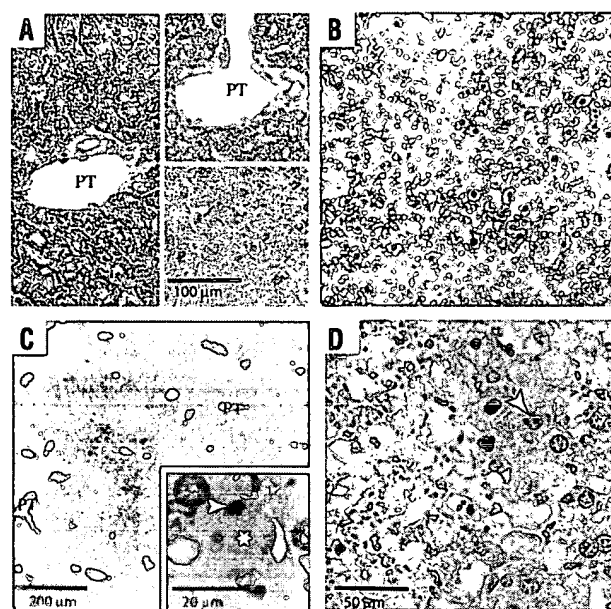


Figure 2. Representative liver sections of transgenic animals. (A) Liver section immunostained with human caspase-3 antibody (Sc-1226, which recognizes both inactive and active forms) before any CID injection. Low inset, nontransgenic animal; high inset, transgenic animal after CID injection, all in the same experimental conditions. Note the absence of staining in endothelial and biliary epithelial cells (original magnification 200 \times). (B) Liver section stained with HE before any CID injection (original magnification 200 \times). (C) Liver section stained with HE 18 h after a 2 mg/kg CID injection, showing >80% of liver destruction (apoptotic areas appear bright red; original magnification 100 \times). Inset: high magnification of the same animal liver section with morphological characteristics of apoptosis such as Councilman bodies (star) or nuclear condensation (arrowhead) (original magnification 1,000 \times). (D) TUNEL analysis of a liver section analyzed 18 h after CID injection. Note positive nuclei stained in dark brown (arrowhead) and surrounding cells already destroyed (original magnification 400 \times). CV, central vein; PT, portal tract.

serum ALT 24 h after the injection. Two transgenic lines (Tg 16 and Tg 22) showed a rapid increase in ALT activities, Tg 22 showing a ninefold higher mean level of ALT ($6,400 \pm 3,184$ IU; $n = 6$) than Tg 16 (730 ± 782 IU; $n = 5$). Therefore, Tg 22 was used for further studies. Histology confirmed hepatocyte damage in injected animals, sparing periportal regions (Fig. 2C). Up to 85% of total hepatocytes were destroyed 18 h after a single AP20187 injection, with morphological characteristics of apoptosis (nuclear condensation, Councilman bodies) shown in Figure 2C. This observation was confirmed by TdT-mediated dUTP nick-end labeling (TUNEL) analysis (Fig. 2D). Apoptosis was still detectable 96 h after the injection of AP20187, and had completely disappeared at day 7. Routine histological examination of other organs (spleen, kidney, gut, brain, lung, and heart) failed to show any specific lesion (data not shown).

Kinetic study of liver damage and regeneration. To study the relationship between the kinetics of human caspase-3 activation and cytolysis, we conducted western blot analyses on the livers of animals submitted to apoptosis. Cleaved M-Fv2-Casp3 could be detected as early as 3 h after the injection of AP20187, when ALT levels were still within the normal range (Fig. 3A). Cleaved bands could still be seen 6, 9, 12, 24, and, very faintly, 96 h after AP20187 injection. Unprocessed protein also remained present at all time points. We confirmed the activation of caspase-3 by measuring the proteolytic cleavage of the Ac-DEVD-AMC fluorogenic substrate by liver protein samples. The increase in M-Fv2-Casp3 activity was detected as early as 6 h after injection, before biochemical evidence of liver cytolysis (Fig. 3B).

The kinetics of liver injury was further evaluated by serum ALT dosage at different times after a single injection of 2 mg/kg of AP20187. Serum ALT started to increase between 6 and 12 h after AP20187 injection, reaching a peak between 12 and 24 h (Fig. 3C) and then returning to the baseline after 72 h. At 18 h after the injection of AP20187, ALT increased up to 400 times the normal value (mean \pm s.d., $10,700 \pm 9,803$; $n = 10$; median 7,000). In contrast, ALT activity remained at basal levels throughout the experiment in non-transgenic littermates injected with AP20187 as well as in transgenic animals injected only with the CID carrier.

The M-F₂-Casp3 activation pattern was studied by immunohistochemistry using an anti-caspase-3 antibody preferentially reacting with processed active human caspase-3 (ref. 26). Before CID injection, a faint staining could be seen around central veins (Fig. 4A). Upon injection, there was a strong membranous and cytoplasmic reinforcement, preferentially in the centrilobular area (Fig. 4B). This zonation corresponded to the apoptotic area observed in standard hematoxylin and eosin (HE) staining (Fig. 2C). Membranous staining is probably due to the myristoylation sequence present in the transgene. Four days after CID injection, only a faint staining could be detected in a few scattered hepatocytes (Fig. 4C). Liver regeneration began 24 h after the apoptotic challenge. Between two and four days, numerous figures of mitosis were observed, mostly around apoptotic areas (Fig. 4D). At day 7, the liver had recovered a normal architecture (Fig. 4E). The percentage of cells entering S phase, expressed as the proportion of BrdU⁺ hepatocyte nuclei at 12, 24, 48, 72, and 96 h, showed an incorporation peak at 48 h and the progressive return to baseline after 96 h (Fig. 4F, G).

Dose dependence of liver injury and re-administration of CID. We monitored the time course of ALT activities after injection of increasing concentrations of the CID. No significant ALT rise could be detected with a dose of 0.01 mg/kg. ALT levels increased significantly ($P < 0.05$) with doses ranging from 0.1 to 2 mg/kg. In animals injected with 10 mg/kg CID, though not significantly higher than with 2 mg/kg, peak ALT level was earlier, between 6 and 12 h, whereas the peak ALT level was ~48 h in animals injected with 0.1 mg/kg CID (not shown). To quantitate these results globally, we calculated the area under the curve (AUC) of ALT variation for each dose of CID (Fig. 5A). We observed significant differences between doses ranging from 0.01 to 0.5 mg/kg with a strong correlation between dose and liver injury (Spearman's $\rho = 0.86$; $P < 0.0001$).

Interestingly, although ALT levels could reach up to 27,000 IU/L, we never observed any mortality in our heterozygous transgenic animals at 2 or 10 mg/kg ($n = 24$). To determine whether a more severe phenotype could be obtained by gene dosage, we bred the animals to homozygosity. In these homozygous animals, 100% mortality ($n = 8$) was observed within 16 h after a 2 mg/kg AP20187 injection and, when moribund animals were euthanized, histology showed total hepatocyte destruction throughout the liver.

Our system allowed multiple injections of CID. We injected heterozygous transgenic animals three times with 0.1 mg/kg AP20187 at one-week intervals and obtained three successive rounds of hepatocellular death as assessed by ALT levels (Fig. 5B).

Feedback loop with cytochrome *c* release in induced livers. Caspase-3 is normally an executing caspase, acting downstream of mitochondria. In our model, caspase-3 is directly activated without the need for upstream mitochondrial events. Previous *ex vivo* observations have suggested the presence of a positive-feedback loop required for apoptosis in hepatocytes, which is initiated by caspase-3-mediated cleavage of upstream proteins such as BID, caspase-9 and caspase-8, Bcl-2 and Bcl-X_L. This leads to a mitochondrial release of cytochrome *c*²⁷⁻²⁹. Therefore, we also studied the kinetics of cytochrome *c* release after AP20187 injection. In untreated transgenic and nontransgenic animals, cytochrome *c* appeared in the

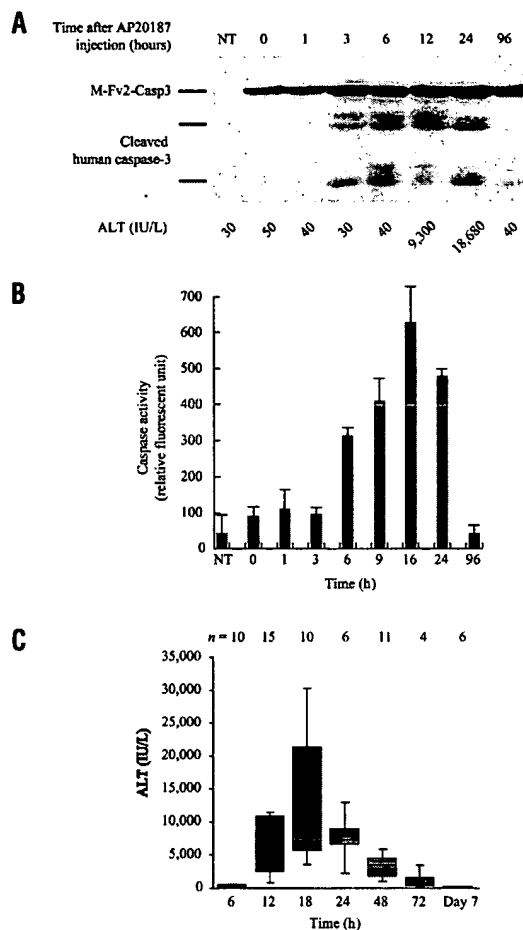


Figure 3. Kinetics of caspase-3 activation and hepatocyte cytolysis in transgenic animals. (A) Western blot analysis of caspase-3 activation in liver samples of nontransgenic (NT) and Tg 22 transgenic animals upon injection of 2 mg/kg CID. Cleaved bands are clearly visualized as soon as 3 h after CID injection. Uncleaved caspase-3 remains at any time. ALT levels of corresponding animals are given below. (B) Fluorometric dosage of caspase-3 activity. Error bars indicate s.e.m. (C) Box plots of ALT values measured at different times after CID injection. The top and bottom of the box are the 25th and 75th percentiles. The line through the box is the median. Bars indicate s.e.m. The number of animals at each time is indicated above.

heavy membrane fraction of the liver (Fig. 6). At 6 h after AP20187 injection, when M-F₂-Casp3 was already cleaved but before serum increases in ALT, cytochrome *c* was detected in the cytoplasmic fraction of the liver (Fig. 6). This result suggests that an upstream event such as cytochrome *c* release is induced *in vivo* by direct caspase-3 activation before definitive cell damage has occurred, and may contribute to the completion of hepatocyte apoptosis in this specific mouse model.

Discussion

Apoptosis is an intracellular process involved in several forms of hepatitis. In these situations, a causal involvement of cytokines such as tumor necrosis factor- α (TNF- α) or CD95-Fas ligand (CD95L) has been described in the initiation of hepatocyte cell death. Both pathways lead ultimately to activation of caspase-3 (refs. 30, 31), the key executioner of the cell death program, which cleaves a number of cellular substrates and orchestrates the morphological and biochemical features of apoptosis.

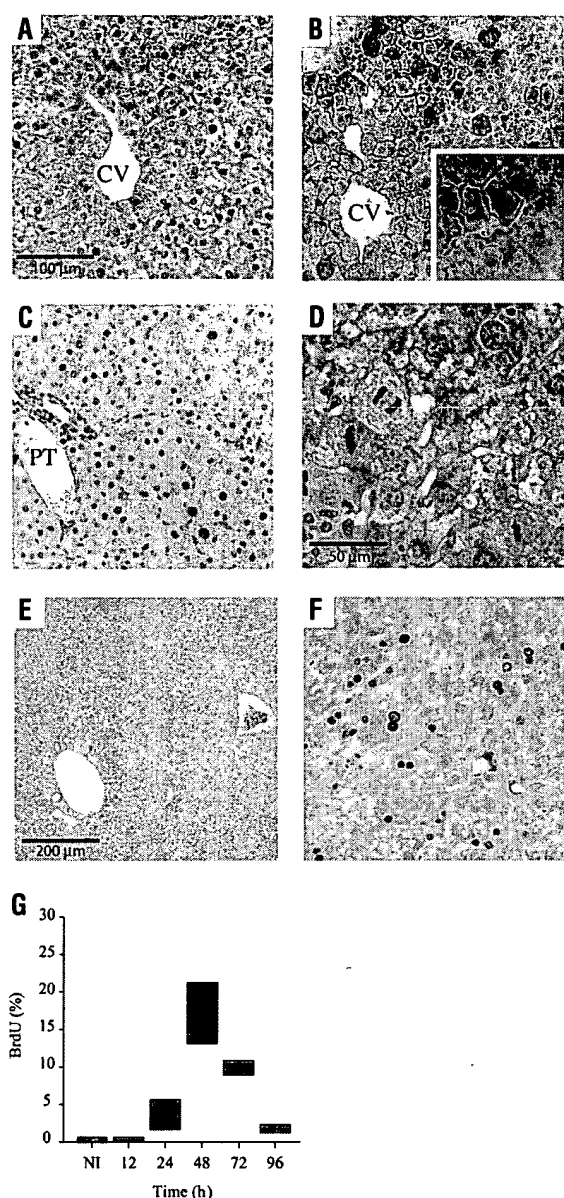


Figure 4. Kinetics of liver damage and regeneration in transgenic animals. (A–C) Liver sections of representative animals before or after a 2 mg/kg CID injection immunostained with DAKO A-3537 anti-human caspase-3 antibody (original magnification 200 \times) at the same time and under identical conditions. (A) Appearance before any CID injection. (B) Appearance 12 h after CID injection. Inset: higher magnification (400 \times) of the same liver section. (C) Appearance at four days after CID injection. (D) HE staining at four days (original magnification 400 \times). (E) HE staining at seven days (original magnification 100 \times). (F) BrdU immunostaining at 72 h (original magnification 200 \times). (G) Box plots of BrdU $^{+}$ hepatocyte percentage at different times after CID injection and for equivalent levels of ALT. Two animals are shown for each time. NI, noninjected.

Here we describe a mouse model of inducible liver injury based on cross-linking a genetically modified procaspase-3 containing two CID-binding domains. The forced dimerization leads to caspase transproteolysis and activation, resulting in hepatocyte apoptosis. CIDs are nontoxic, lipid-permeable ligands that can be administered intravenously, intraperitoneally, or even orally, and that are neither immunogenic nor immunosuppressive.

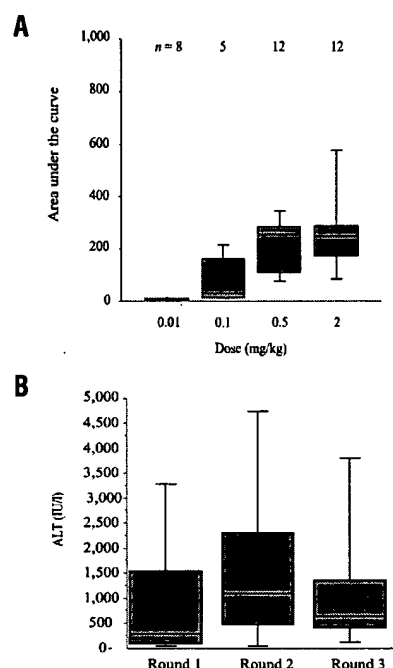


Figure 5. Dose dependence and CID re-injection. (A) Area under the curve (AUC) of ALT variations after the injection of increasing doses of CID. The number of mice used in each group is shown above. (B) Box plots of ALT values measured 48 h after three successive 0.1 mg/kg CID injections ($n = 9$). There is no statistical difference between each round.

We obtained four transgenic mouse lines expressing the inactive chimeric procaspase-3 specifically in hepatocytes. We detected the protein in the liver of all lines at various levels. Only the lines with the highest level of M-F₂-Casp3 expression showed considerable hepatitis after CID injection, suggesting that M-F₂-Casp3 activation is dependent on its level of expression. There is probably a critical threshold of M-F₂-Casp3 expression at the cellular level to allow efficient activation by CID. This hypothesis was reinforced by the observation of a more severe phenotype in homozygous transgenic animals and emphasizes the need for a strong promoter to achieve efficient cell ablation with this system.

In the absence of CID, the liver was normal, without any biochemical evidence of cytolysis, underlining the absence of leakiness of the system. Upon activation, the animals showed dose-dependent liver apoptosis, with the severity of liver injury being tightly correlated to the level of ALT. The lesions spared the periportal regions in heterozygous mice and destroyed the entire lobule in homozygous mice, leading to FHF and death in the latter group.

The absence of mortality in heterozygous animals showing as high as 85% of hepatocyte destruction contrasts with other models of liver injury in which substantial mortality has been reported with similar levels of destruction. This could be explained by the absence of nonparenchymal toxicity in our strategy compared with other models^{14,32}.

One week after injection of CID, the liver had completely regenerated and showed a normal architecture. Hepatocyte DNA synthesis peaked 48 h after the apoptotic challenge, as has been observed with two-thirds partial hepatectomy, the most common method used to study liver regeneration.

Our approach to conditional hepatocyte ablation has distinct advantages over and differences from previous methods. Cytotoxicity is not detectable in the uninduced state, in contrast to what has been described when expressing the gene encoding DT-A

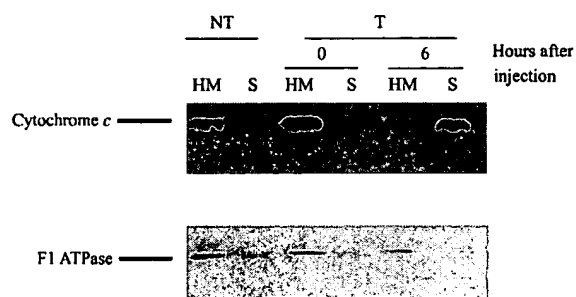


Figure 6. Cytochrome *c* release in the liver of CID-injected mice. Cytosolic (S) and heavy membranes (HM) liver fractions from nontransgenic (NT) or transgenic (T) mice before injection (0) and 6 h (6) after a 2 mg/kg CID injection. F1 ATPase is used as an internal control of a heavy membrane protein.

under the control of a tetracycline-regulatable promoter³³. Upon injection of the CID, ablation is highly efficient, dose-dependent, and without toxicity to other cells or bystander effect³⁴. Cell death relies upon a pure cytolytic process. This latter point differs from the gancyclovir–thymidine kinase approach, in which mice die in 24 days after induction, principally from chronic liver injury rather than acute cytolysis.

The model of transgenic mice expressing human chimeric procaspase-3 specifically in the liver should have broad applicability. First, it provides a pertinent model of liver injury and FHF, offering a useful tool to study liver regeneration and stem cell plasticity in a clinically relevant context. Second, it can be used to study apoptosis *in vivo*. We describe here, for example, that the elective *in vivo* activation of M-F₂-caspase-3 in hepatocytes leads to cytochrome *c* release before any substantial liver injury. Therefore, there is a positive-feedback loop in which caspase-3 acts both upstream to commit the cell irreversibly to programmed death, and downstream to trigger its execution. Finally, our model will be useful for selective repopulation of the livers of mice with human hepatocytes, a situation that cannot be obtained in the DT-receptor ablation model, because human cells are highly sensitive to this toxin. Although it has been shown that transgenic animals expressing urokinase in the liver demonstrate considerable liver repopulation with human hepatocytes³⁵, this transgenic model is not inducible and shows a high level of perinatal lethality. Our model should bypass these difficulties.

Our method could be generalized to other cell types because it targets the apoptotic pathway, a physiological process that has been described in numerous pathological circumstances such as type I diabetes³⁶ or end-stage failing human cardiomyopathy³⁷. Useful animal models of these disorders can be created with this approach by targeting pancreatic β cells or cardiomyocytes, respectively.

Experimental protocol

Generation of *TTR-Casp3* transgenic mice. The 1.6 kb *NotI*–*EcoRI* of *M-F₂-Casp3-E* (ref. 23) from *pSH1/M-Fv2-Yama-E* was blunt-ended with Klenow fragment of DNA polymerase I and ligated into a unique *StuI* site located in the second exon of the *pTTR-ExV3* vector²⁴ (Fig. 1A). The 4.6 kb *HindIII* fragment containing the 3 kb *TTR* promoter driving the chimeric *M-F₂-Casp3-E* cDNA (*TTR-Casp3*) was injected into the pronuclei of B6D2 fertilized eggs.

Northern blot analysis. Total RNA was extracted from homogenized tissues using the guanidium thiocyanate procedure³⁸. A 10 μ g sample of total RNA was fractionated through 1.5% (wt/vol) agarose–formaldehyde gels, transferred to Hybond-N⁺ membranes, and probed with the *TTR-Casp3* sequence.

Western blot analysis. Total liver protein was isolated from snap-frozen tissue by homogenization in 5% (wt/vol) 2X Laemmli sample buffer (Sigma, St.

Louis, MO), resolved in 12% (wt/vol) SDS–polyacrylamide gel, and transferred to a nitrocellulose filter. Membranes were immunoblotted with an anti-caspase-3 goat primary antibody (RD Systems, Minneapolis, MN) at a dilution of 1:400, revealed with a peroxidase-coupled anti-goat IgG. All immunoblots were visualized by chemiluminescence (ECL Amersham Biosciences, Piscataway, NJ) and normalized with an anti-actin antibody (Santa Cruz Biotechnology, Santa Cruz, CA).

Animal procedures. All animal procedures were in accordance with European guidelines for the care and use of laboratory animals. Some animals were euthanized when moribund. Lyophilized AP20187 (ARIAD Pharmaceuticals, Cambridge, MA) was solubilized as recommended by the manufacturer. We administered AP20187 by intraperitoneal injection in a total volume of 200 μ l per injection.

Measurement of hepatocyte proliferation, histology, immunohistochemistry. Cell proliferation was assessed by bromodeoxyuridine (BrdU) (Sigma-Aldrich, St. Louis, MO) incorporation into nuclei. Animals were given a 2 h pulse of 50 mg/kg BrdU before their death. The livers were perfused with neutral saline and subjected to biochemical and immunohistochemical analyses. Liver samples fixed in 10% phosphate-buffered formalin were embedded in paraffin. Thin (3 μ m) sections were stained with HE for standard microscopy. BrdU immunohistochemistry was carried out after a 30 min incubation at 37°C with 20 μ g/ml proteinase K and a 30 min incubation at 37°C with 2 M HCl. Sections were then rinsed in PBS three times for 5 min each, and incubated overnight with a biotinylated monoclonal primary antibody (Clone Bu20a; DAKO, Glostrup, Denmark). Immunostaining was revealed with the ARK kit (DAKO) according to the manufacturer's instructions. The proportion of BrdU⁺ nuclei was determined by counting at least 1,000 cells in 10–20 random fields at 400 \times magnification in two different lobes.

For caspase-3 immunohistochemistry, goat anti-human caspase-3 (cat. no. sc-1226; Santa Cruz Biotechnology) and rabbit anti-human caspase-3 (cat. no. A-3537; DAKO) were used at a dilution of 1:200 for 1 h at room temperature. Slides were developed with the appropriate secondary antibody revealed with peroxidase and diaminobenzidine followed by counterstaining with hematoxylin. TUNEL staining was done on deparaffinized tissue sections with the Apoptag system according to the manufacturer's instructions (Intergen, Purchase, NY).

Caspase activity. Liver lysates were prepared by homogenization in hypotonic buffer (25 mM HEPES, pH 7.5, 5 mM MgCl₂, 1 mM EGTA, 1 mM phenylmethylsulfonyl fluoride (PMSF), 1 mg/ml leupeptin and aprotinin). Homogenates were centrifuged at 15,000 r.p.m. for 15 min, and extracted proteins (50 μ g) were tested in duplicate experiments by measuring the proteolytic cleavage of specific fluorogenic substrate of Ac-DEVD-AMC for caspase-3 (CaspACE Assay System; Promega, Madison, WI).

Analysis of cytochrome *c* release. Liver homogenates were prepared and subfractionated as described³⁹. Both mitochondria and cytosol extracts were analyzed by 15% SDS–PAGE followed by western blotting with an anti-cytochrome *c* antibody (PharMingen, San Diego, CA) at a dilution of 1:200 and an anti-F1 ATPase at a dilution of 1:3,000 (gift of J. Lunardi, Faculty of Medicine, Grenoble, France) as a mitochondrial control.

Serum biochemical analysis. Blood samples were collected by retro-orbital puncture at different times after AP20187 injection. Serum samples were collected by centrifugation of collected blood, and the catalytic activity of ALT was determined at 30°C according to the IFCC method using a ALAT/GPT kit (Roche, Mannheim, Germany) on a Hitachi 747 analyzer (Tokyo, Japan).

Data analysis. All values are expressed as mean \pm s.d. ALT was considered as a continuous variable, and total liver injury was estimated with the AUC. Correlation between groups was done using Spearman's ρ . Data sets were compared with ANOVA and Student's *t*-test for unpaired data when appropriate.

Acknowledgments

We thank Terry Van Dyke for the *TTR* vector and ARIAD Pharmaceuticals for providing us with AP20187 (www.ariad.com/regulationkits). We also thank Eva Mezey for proofreading the manuscript.

Competing interests statement

The authors declare that they have no competing financial interests.

Received 3 May 2002; accepted 2 October 2002

1. Galle, P. R. *et al.* Involvement of the CD95 (APO-1/Fas) receptor and ligand in liver damage. *J. Exp. Med.* **182**, 1223–1230 (1995).
2. Nanji, A. A. Apoptosis and alcoholic liver disease. *Semin. Liver Dis.* **18**, 187–190 (1998).
3. Fox, C. K., Furtwaengler, A., Nepomuceno, R. R., Martinez, O. M. & Krams, S. M. Apoptotic pathways in primary biliary cirrhosis and autoimmune hepatitis. *Liver* **21**, 272–279 (2001).
4. Strand, S. *et al.* Hepatic failure and liver cell damage in acute Wilson's disease involve CD95 (APO-1/Fas) mediated apoptosis. *Nat. Med.* **4**, 588–593 (1998).
5. Rudiger, H. A. & Clavien, P. A. Tumor necrosis factor- α , but not Fas, mediates hepatocellular apoptosis in the murine ischemic liver. *Gastroenterology* **122**, 202–210 (2002).
6. Patel, T., Roberts, L. R., Jones, B. A. & Gores, G. J. Dysregulation of apoptosis as a mechanism of liver disease: an overview. *Semin. Liver Dis.* **18**, 105–114 (1998).
7. Lee, W. M. Acute liver failure. *N. Engl. J. Med.* **329**, 1862–1872 (1993).
8. Fingerote, R. J. & Bain, V. G. Fulminant hepatic failure. *Am. J. Gastroenterol.* **88**, 1000–1010 (1993).
9. Caraceni, P. & Van Thiel, D. H. Acute liver failure. *Lancet* **345**, 163–169 (1995).
10. Fausto, N. Liver regeneration. *J. Hepatol.* **32**, 19–31 (2000).
11. Kosai, K., Matsumoto, K., Funakoshi, H. & Nakamura, T. Hepatocyte growth factor prevents endotoxin-induced lethal hepatic failure in mice. *Hepatology* **30**, 151–159 (1999).
12. Hecht, N. *et al.* Hyper-IL-6 gene therapy reverses fulminant hepatic failure. *Mol. Ther.* **3**, 683–687 (2001).
13. Kobayashi, N. *et al.* Prevention of acute liver failure in rats with reversibly immortalized human hepatocytes. *Science* **287**, 1258–1262 (2000).
14. Newsome, P. N., Plevris, J. N., Nelson, L. J. & Hayes, P. C. Animal models of fulminant hepatic failure: a critical evaluation. *Liver Transpl.* **6**, 21–31 (2000).
15. Palmiter, R. D. *et al.* Cell lineage ablation in transgenic mice by cell-specific expression of a toxin gene. *Cell* **50**, 435–443 (1987).
16. Behringer, R. R., Mathews, L. S., Palmiter, R. D. & Brinster, R. L. Dwarf mice produced by genetic ablation of growth hormone-expressing cells. *Genes Dev.* **2**, 453–461 (1988).
17. Braun, K. M., Degen, J. L. & Sandgren, E. P. Hepatocyte transplantation in a model of toxin-induced liver disease: variable therapeutic effect during replacement of damaged parenchyma by donor cells. *Nat. Med.* **6**, 320–326 (2000).
18. Matthews, T. & Boehme, R. Antiviral activity and mechanism of action of ganciclovir. *Rev. Infect. Dis.* **10**, S490–S494 (1988).
19. Culver, K. W. *et al.* In vivo gene transfer with retroviral vector-producer cells for treatment of experimental brain tumors. *Science* **256**, 1550–1552 (1992).
20. Saito, M. *et al.* Diphtheria toxin receptor-mediated conditional and targeted cell ablation in transgenic mice. *Nat. Biotechnol.* **19**, 746–750 (2001).
21. Kobayashi, K. *et al.* Immunotoxin-mediated conditional disruption of specific neurons in transgenic mice. *Proc. Natl. Acad. Sci. USA* **92**, 1132–1136 (1995).
22. Collier, R. J. in *ADP-Ribosylating Toxins and G Proteins: Insights into Signal Transduction* (eds. Moss, J. & Vaughan, M.) 3–19 (American Society for Microbiology, Washington, DC, 1990).
23. Fan, L., Freeman, K. W., Khan, T., Pham, E. & Spencer, D. M. Improved artificial death switches based on caspases and FADD. *Hum. Gene Ther.* **10**, 2273–2285 (1999).
24. Yan, C., Costa, R. H., Darnell, J. E. Jr., Chen, J. D. & Van Dyke, T. A. Distinct positive and negative elements control the limited hepatocyte and choroid plexus expression of transthyretin in transgenic mice. *EMBO J.* **9**, 869–878 (1990).
25. Clackson, T. *et al.* Redesigning an FKBP-ligand interface to generate chemical dimerizers with novel specificity. *Proc. Natl. Acad. Sci. USA* **95**, 10437–10442 (1998).
26. Krajewska, M. *et al.* Immunohistochemical analysis of *in vivo* patterns of expression of CPP32 (Caspase-3), a cell death protease. *Cancer Res.* **57**, 1605–1613 (1997).
27. Cheng, E. H. *et al.* Conversion of Bcl-2 to a Bax-like death effector by caspases. *Science* **278**, 1966–1968 (1997).
28. Woo, M. *et al.* In vivo evidence that caspase-3 is required for Fas-mediated apoptosis of hepatocytes. *J. Immunol.* **163**, 4909–4916 (1999).
29. Slee, E. A., Keogh, S. A. & Martin, S. J. Cleavage of BID during cytotoxic drug and UV radiation-induced apoptosis occurs downstream of the point of Bcl-2 action and is catalysed by caspase-3: a potential feedback loop for amplification of apoptosis-associated mitochondrial cytochrome *c* release. *Cell Death Differ.* **7**, 556–565 (2000).
30. Jones, R. A. *et al.* Fas-mediated apoptosis in mouse hepatocytes involves the processing and activation of caspases. *Hepatology* **27**, 1632–1642 (1998).
31. Zheng, T. S. *et al.* Caspase-3 controls both cytoplasmic and nuclear events associated with Fas-mediated apoptosis *in vivo*. *Proc. Natl. Acad. Sci. USA* **95**, 13618–13623 (1998).
32. Janin, A. *et al.* CD95 engagement induces disseminated endothelial cell apoptosis *in vivo*: immunopathologic implications. *Blood* **99**, 2940–2947 (2002).
33. Lee, P. *et al.* Conditional lineage ablation to model human diseases. *Proc. Natl. Acad. Sci. USA* **95**, 11371–11376 (1998).
34. Xie, X. *et al.* Adenovirus-mediated tissue-targeted expression of a caspase-9-based artificial death switch for the treatment of prostate cancer. *Cancer Res.* **61**, 6795–6804 (2001).
35. Mercer, D. F. *et al.* Hepatitis C virus replication in mice with chimeric human livers. *Nat. Med.* **7**, 927–933 (2001).
36. Yoon, J. W. & Jun, H. -S. Cellular and molecular pathogenic mechanisms of insulin-dependent diabetes mellitus. *Ann. NY Acad. Sci.* **928**, 200–211 (2001).
37. Narula, J. *et al.* Apoptosis in heart failure: release of cytochrome *c* from mitochondria and activation of caspase-3 in human cardiomyopathy. *Proc. Natl. Acad. Sci. USA* **96**, 8144–8149 (1999).
38. Chirgwin, J. M., Przybyla, A. E., MacDonald, R. J. & Rutter, W. J. Isolation of biologically active ribonucleic acid from sources enriched in ribonuclease. *Biochemistry* **18**, 5294–5299 (1979).
39. Gross, A. *et al.* Caspase-cleaved BID targets mitochondria and is required for cytochrome *c* release, while BCL-XL prevents this release but not tumor necrosis factor-R1/Fas death. *J. Biol. Chem.* **274**, 1156–1163 (1999).